Journal of Alloys and Compounds 591 (2014) 29–33

Contents lists available at ScienceDirect

Journal of Alloys and Compounds

journal homepage: www.elsevier.com/locate/jalcom

Influence of Ni on the magnetocaloric effect in Nanoperm-type soft-magnetic amorphous alloys

B. Podmiljsak [a,c,*], J.-H. Kim [b], P.J. McGuiness [a,c], S. Kobe [a]

[a] Department for Nanostructured Materials, Jozef Stefan Institute, Jamova cesta 39, 1000 Ljubljana, Slovenia
[b] Analysis Research Devision, Korea Basic Science Institute, 1370, Sankyuk-Donk, Buk-gu, Daegu, Republic of Korea
[c] Center of Excellence NAMASTE, Ljubljana, Jamova cesta 39, 1000 Ljubljana, Slovenia

ARTICLE INFO

Article history:
Received 11 July 2013
Received in revised form 13 December 2013
Accepted 16 December 2013
Available online 28 December 2013

Keywords:
Amorphous materials
Rapid-solidification
Magnetization
Magnetocaloric effect
Refrigerant capacity
Curie temperature

ABSTRACT

We have studied the influence of Ni on the magnetocaloric effect (MCE) in Nanoperm-type amorphous materials by investigating a series of $Fe_{84-x}Ni_xZr_6B_{10}$ alloys with $x = 0$, 2, 4 and 6. As expected, the Curie temperature increased with the amount of Ni from 427 K for $x = 0$ to 482 K for $x = 6$. The maximum magnetic entropy change (ΔS_M^{pk}) for an applied field of 1.4 T also increased, reaching a value of 1.52 J/K kg for $x = 6$, which is an increase of 25% compared to the Ni-free alloy. The refrigerant capacity first decreased for $x = 2$ and then increased, reaching a maximum value of 93 J/kg ($\Delta H = 1.4$ T) for $x = 6$. For a 5 T field change, the value increased to 407 J/kg, which is higher than the 355 J/kg achieved with $Gd_5Ge_{1.9}Si_2Fe_{0.1}$. We confirmed the proposed "master curve" behavior for second-order magnetic transition (SOMT) alloys for the temperature dependence of ΔS_M for different alloy compositions of the same series, which makes it easier and faster to find proper candidates for a magnetic refrigerator.

1. Introduction

Iron-based amorphous alloys have received a great deal of attention since their discovery in the 1960s [1], because of their excellent soft-magnetic properties and their consequent use in electronic devices such as transformer cores. However, they have only recently drawn attention as a working material for room-temperature magnetic refrigerators, where they have a number of advantages over already known magnetocaloric materials [2–7]. Magnetic refrigerators work on the principle of the magnetocaloric effect [8], which involves the temperature change of a magnetic material upon the application of a magnetic field. When magnetized, the entropy of the spin subsystem is decreased and, under adiabatic conditions, the transfer of energy to the lattice induces heating of the material. Conversely, the adiabatic demagnetization of the material causes its cooling.

Until now, materials with a first-order magnetic transition (FOMT), like $Gd_5(Si,Ge)_4$ [9], $La(Fe,Si)_{13}$ [10], FeMnPAs [11], $Ni_2(Mn,Ga)$ [12] and others [13], have been considered the best choice for magnetic refrigerators because of their very large (ΔS_M^{pk}), which occurs as a result of a coupled magneto-structural transition. But these structural changes also present some drawbacks. They have very large thermal and magnetic-field hysteresis, which can be reduced by substituting alternative elements, but only at the expense of a lower ΔS_M [14]. Furthermore, because of the structural transition, large volume changes and stresses between the coexisting phases appear, which make the sample very brittle [15]. The operating temperature range also tends to be very narrow and some of the proposed materials contain toxic elements.

Materials with a SOMT lack the very large ΔS_M^{pk}, but they do have a very high refrigeration capacity (RC), which is now recognized as the key parameter, because it is a better way by which to compare different MC materials. The other positive characteristics of SOMT materials are a low magnetic hysteresis, a high electrical resistivity, enhanced corrosion resistance, good mechanical properties, and a T_C tunable by varying the composition [3,7]. Fe-based amorphous magnetocalorics also have the advantage of generally being very cheap and easy to produce. What tends to limit their use is the high Curie point of the alloys, and attempts to change the composition in order to reduce the T_C usually also reduce the magnetic moment, which then negatively affects the magnetocaloric effect. There have been suggestions to use these alloys in high temperature applications [4,16], but the primary goal remains a useful magnetocaloric effect at room temperature. In this paper the focus is on substituting nickel for iron in Fe–Zr–B alloys and its effect on the magnetic properties. Not many papers have been published where they used Ni to modify the MCE of Fe-based amorphous

* Corresponding author at: Department for Nanostructured Materials, Jozef Stefan Institute, Jamova cesta 39, 1000 Ljubljana, Slovenia. Tel.: +386 14773818.
E-mail address: Benjamin.podmiljsak@ijs.si (B. Podmiljsak).

0925-8388/$ - see front matter © 2013 Elsevier B.V. All rights reserved.
http://dx.doi.org/10.1016/j.jallcom.2013.12.150

materials [7,17,18]. Our results show that nickel increases the magnetocaloric effect, the RC and the Curie temperature, but not in a linear fashion as is observed with other alloys [7].

2. Experiment

We studied samples with the compositions $Fe_{84-x}Ni_xZr_6B_{10}$ (x = 0, 2, 4 and 6). Button ingots where prepared with an Edmund Bühler AM4 Arc Melter. These where then melt spun by inductively melting the button ingots in a partial argon atmosphere and ejecting the melt through a 0.6-mm orifice onto the perimeter of a copper wheel rotating at a surface speed of 50 m s^{-1} with an Edmund Bühler ST1 Melt Spinner. The ribbons produced with this equipment where 2 mm wide and 25 μm thick. The crystal structure of the as-spun ribbons surface was examined by X-ray diffraction (XRD) using a Siemens D5000 diffractometer with Cu Kα radiation (2θ = 5–80°). All the samples were cross-sectioned, and then polished for the JEOL JSM-7600F FEG-SEM and quantitatively assessed in terms of their composition with EDS.

The magnetic properties were measured on a LakeShore vibrating-sample magnetometer (Model 7303) with a heater attached. To determine the MCE and the refrigeration capacity the magnetization was measured at discrete magnetic-field values between 0 and 1.4 T at constant temperature. This was then repeated at different temperatures, and from the magnetic measurements the ΔS_M was calculated using an approximation of Maxwell's relation:

$$\Delta S_M \approx \frac{1}{\Delta T}\left[\int_0^{H'} M(T+\Delta T,H)dH - \int_0^{H'} M(T,H)dH\right] \quad (1)$$

3. Results and discussion

The ribbons produced with the melt spinner are on the average 2 mm wide and 25 μm thick, while because of the amorphous elastic nature being endless in length. The amorphous structure of the melt-spun ribbons was also confirmed by XRD. Over a wide 2θ range of 10–80° only a broad peak is seen, without any trace of sharp peaks related to a periodic lattice structure. All four specters are presented in Fig. 1. Also the images of the electron microscope showed that the ribbons are uniform with no secondary phase present. Fig. 2 shows the SEM images of ribbon x = 2. The EDS results show the same stoichiometry after the melt spinning as the weight material. This shows that there were no losses of material during sample preparation. Table 1 shows the EDS results for all four samples. Additional to the center of the ribbon we measured also the composition close to the surface. When melt spinning the surface touching the wheel cools down faster than the one exposed to argon, which can lead to a change in composition. The numbers show that this did not occur in our case.

Fig. 3 shows the thermomagnetic measurements conducted on the samples. The Curie temperature for the base alloy is at 427 K. Adding nickel shifts the Cure temperature and the magnetic response to higher values. For x = 2, 4 and 6 the values of the Curie temperatures are 465 K, 473 K and 482 K, respectively.

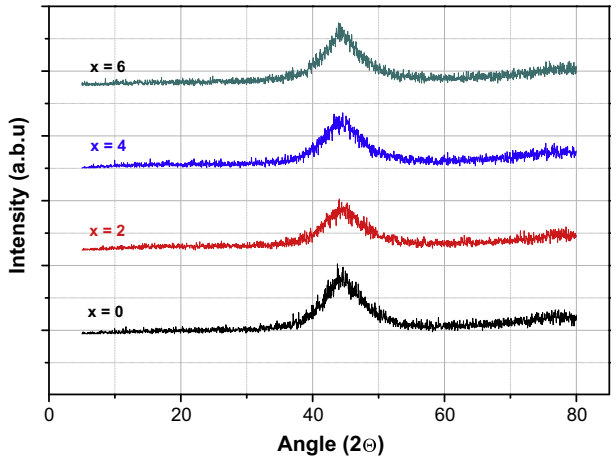

Fig. 1. XRD patterns of $Fe_{84-x}Ni_xZr_6B_{10}$ (x = 0, 2, 4 and 6).

The change in the magnetic entropy was calculated from the magnetic data, where we can use the Maxwell equation without any need to consider false calculations as when calculating the magnetic entropy change for a first-order magnetic transition (where the Clausius–Clapeyron equation is more suitable) [19]. The temperature dependence of the magnetic entropy change is presented in Fig. 4.

While all the curves show similar shapes, we can see how large an effect nickel has on the Fe–Zr–B alloy. Nickel increases the peak temperature of the magnetic entropy change, due to an increase of the Curie temperature of the alloy. It is well known that small additions of nickel increase the T_C of ferromagnetic amorphous alloys, which can be explained by the contribution of the Fe–Ni interaction (which is thought to be larger than the Fe–Fe interaction, according to the average molecular model) and the change of the non-collinear spin structures of the parent Fe–Zr–B alloy, so a more stable "ferromagnetic" alloy is made with its spin structure approaching a parallel alignment [20]. The Curie temperature is expected to increase up to a substitution of 50 at.% of Fe with Ni, after that it should fall quite rapidly [21]. The Fe–Ni interaction also affects the magnetic moment, which increases with increasing nickel content and is also reflected in the increase in the magnetic entropy change.

Franco et al. showed in magnetocaloric materials with a SOMT that there is a "master-curve" behavior of the magnetic-entropy-change curves not only for the same alloy at different fields, but also for different alloy compositions of the same series [22]. To obtain this master curve we have to rescale the normalized $\Delta S_M(T)$ curves versus a temperature axis in a different way below and above the Curie temperature of the sample by ensuring that the position of two additional reference points on the curve correspond to $\theta = \pm 1$:

$$\theta = \begin{cases} -T - T_{\text{Curie}}/(T_{r1} - T_{\text{Curie}}), & T \leqslant T_{\text{Curie}} \\ (T - T_{\text{Curie}})/(T_{r2} - T_{\text{Curie}}), & T > T_{\text{Curie}} \end{cases},$$

where T_{r1} and T_{r2} are the temperatures of the two reference points, which have been selected as those corresponding to $(1/2)\Delta S_M^{pk}$. Fig. 5 shows the master-curve behavior of the magnetic entropy change for the investigated alloys. It is clear that all the curves fit onto the master curve, confirming the findings in [21].

To calculate the RC from the ΔS_M curves, different methods are used, which makes it hard to compare the values from different authors. We will calculate the RC in two different ways. In the first method [23], the RC values were obtained by numerically integrating the area under the ΔS_M versus T curves, using the temperatures at half-maximum of the ΔS_M peak as the integration limits (RC_{AREA}). In the second method, we used the method of Wood and Potter (RC_{WP}) [24], which is the most commonly used by today's authors. They defined the refrigerant capacity for a reversible refrigeration cycle operating between T_{hot} (the temperature of the hot reservoir) and T_{cold} (the temperature of the cold reservoir) as $RC_{WP} = \Delta S_M \Delta T$, where ΔS_M is the magnetic entropy change at the hot and cold ends of the cycle (defined equal) and $\Delta T = T_{hot} - T_{cold}$. This represents the largest rectangle that can be inscribed inside the $\Delta S_M(T)$ curve.

The refrigerant capacity calculated using the method of wood and potter for the studied alloys is presented in Fig. 6. The graph shows the RC_{WP} as a function of the cold reservoir temperature T_{cold}. The maximum in the RC_{WP} curve represents the optimum working conditions for the refrigeration cycle. It is clear that the substitution with Ni increases the RC_{WP}, along with ΔS_M^{pk}, for the samples x = 4 and x = 6. Increasing ΔS_M^{pk} can have also a negative effect on the RC_{WP} [16], because the shape of the $\Delta S_M(T)$ curve